Bent and Linear Forms of the (μ-Oxo)bis[trichloroferrate(III)] Dianion: An Intermolecular Effect − Structural, Electronic and Magnetic Properties

Agustí Lledós,*[a] Marcial Moreno-Mañas,*[a] Mariona Sodupe,[a] Adelina Vallribera,[a] Ignasi Mata,[b] Benjamín Martínez,[b] and Elies Molins*[b]

Keywords: Iron / Oxygen / (μ-Oxo)trichloroferrate dianion / Packing effects / Magnetic properties / DFT calculations

We have analyzed the great diversity of Fe–O–Fe angles, 140–180°, found in the X-ray structures of the (μ-oxo)bis-[trichloroferrate(III)] dianion $[Cl_3FeOFeCl_3]^{2-}$ from both experimental and theoretical points of view. Theoretical calculations show that only the linear isomer is found as a minimum on the potential energy surface. Detailed analysis of the crystal packing indicates that the angular form is due to attractive intermolecular interactions. Analysis of a selected reduced set of the 45 crystal structures retrieved from the Cambridge Structural Database allowed us to classify the bending of the $[Cl_3FeOFeCl_3]^{2-}$ dianion in three categories, depending on the balance and strength of the intermolecular O···H–X contacts. A crystal diffraction study on the bis(benzyltrimethylammonium) salt has shown both bent (144.6°) and linear (180°) forms of the (μ-oxo)bis[trichloroferrate(III)] dianion. The magnetic susceptibility of this compound has been fitted by assuming two equally weighted contributions (J_{ang} and J_{lin}) of the two forms, considering $J_{ang} - J_{lin}$ estimated by theoretical calculations. The obtained J_{ang} and J_{lin} of −117 and −133 cm^{-1} respectively, agree well with B3LYP results.

Introduction

Understanding spin coupling in condensed matter is of fundamental interest. Strategies to control this coupling are of paramount importance for several material applications. Colossal magnetoresistive manganites, high T_c superconductors or superparamagnetic clusters like Fe8 and Mn12 are impressive examples of how spin coupling can be fine-tuned to promote outstanding material properties.

Uncoupled transition metal atoms with unpaired electrons behave as paramagnets. When two atoms interact, the most stable ground state usually corresponds to the singlet $S = 0$ state. In metals and alloys, the metal atoms are directly linked, but in ceramic materials they are usually bridged by other atoms. Oxygen is a very suitable bridging atom; it is a two-electron acceptor, and its flexibility allows the transformation of a linear into a square configuration. The very simple M−O−M system is ideal to study the spin coupling between metal atoms through a bridging atom, acting as a model for more complicated systems.

In particular, oxo-bridged iron(III) complexes have received considerable attention as both simple and useful models for non-heme metalloproteins containing dinuclear iron units in their active site,[1,2] and in studies of the intramolecular antiferromagnetic spin exchange coupling between two high-spin ferric ions.[1,3,4] Within this family, the (μ-oxo)bis[trichloroferrate(III)] dianion **1** (Figure 1) is ubiquitous. X-ray diffraction studies on salts of **1** have been described with various different cations.[3,5−7] An interesting feature of the crystal structure determinations is that the Fe−O−Fe angle in the solid state ranges from 180 to ca. 140° depending on the respective countercation (Figure 1). In general, bent structures **1a** have been considered for the anions with Fe−O−Fe angles of 146−171°. The apparently linear conformations **1b** (Fe−O−Fe 180°) found in a few cases have been attributed to orientational disorder.[3] In spite of the different Fe−O−Fe angles found in these structure determinations, only one type of anion (i.e. with a unique angle) was found in each crystal.

Interest in (μ-oxo)bis[trichloroferrate(III)] salts has been renewed by the discovery that the two different forms (bent

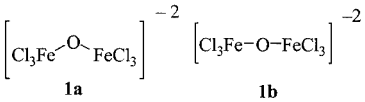

1a **1b**

$[PhCH_2N(CH_3)_3]_2\ [Fe_2OCl_6]$

2

Figure 1. Compound **2** with coexisting bent **1a** and linear **1b** anions

[a] Department of Chemistry, Universitat Autònoma de Barcelona
Cerdanyola, 08193 Barcelona, Spain
Fax: (internat.) + 34-93/5811265
E-mail: marcial.moreno@uab.es
agusti@klingon.uab.es
[b] Institut de Ciència de Materials de Barcelona (CSIC),
Campus de la UAB, 08193 Bellaterra, Barcelona, Spain
E-mail: elies.molins@icmab.es

and linear) can be simultaneously present in the crystal. A crystal diffraction study on the bis(benzyltrimethylammonium) salt **2** showed that both bent (144.6°) and linear (180°) anions were present in the solid, in a ratio of 1:1.[8] Instead of a linear arrangement, the elongated shape of the ellipsoids at the oxygen atoms is also compatible with the presence of two angular conformers (> 165°). However, the ellipsoids' shape, which could be due to either vibrational behavior or some disorder between two quasi-linear conformers, was not explained. In any case, Mössbauer spectroscopy of **2** showed a doublet exhibiting notorious peak asymmetry. The spectrum was fitted with two symmetric doublets associated with two different environments for the iron atoms in the crystal.[8] Thus, from crystal structure and Mössbauer spectroscopy two different Fe−O−Fe forms were identified. Recently, two different types of crystals were obtained for tetramethylformamidinium disulfide (μ-oxo)bis[trichloroferrate(III)] (Form I: orthorhombic; Form II: monoclinic).[9] Two independent (μ-oxo)bis[trichloroferrate(III)] ions, with Fe−O−Fe angles of 146.4 and 180°, were found in the asymmetric unit of Form I, whereas only one ion (Fe−O−Fe 167.9°) was found in Form II. The Fe−O−Fe antisymmetric vibrations in the IR spectra, at 845 and 890 cm^{-1} for Form I crystals and 875 cm^{-1} for Form II crystals, are consistent with such variations in the Fe−O−Fe bond angles.[9]

The concurrent presence of both bent and linear forms of anion **1** in the same crystal raises the possibility of two minima on the Fe−O−Fe potential energy curve. Moreover, given the small separation between the low-spin ground state ($S = 0$) and the high-spin excited state ($S = 5$), the two minima might be spin isomers, corresponding to antiferromagnetic and ferromagnetic couplings of the $S = 5/2$ Fe^{III} spins, respectively.

The magnetic properties of (μ-oxo)bis[trichloroferrate(III)] salts have been extensively studied,[1,3] but in all cases only one anion was present. Therefore, we decided to study the magnetism of two coexisting $[Cl_3FeOFeCl_3]^{2-}$ anions. In the early 1990s a systematic theoretical study on the geometry dependence of the magnetic exchange constant J of $[Fe_2OCl_6]^{2-}$ was performed by means of UHF calculations.[10] Nowadays, quantitative calculations of the exchange coupling constants in dinuclear transition metal complexes are possible. The application of broken symmetry DFT calculations produces very good estimates of J, as compared to experimental data.[11] However, in most calculations the magnetic coupling constant is related to the singlet/triplet energy difference. In the (μ-oxo)bis[trichloroferrate(III)] anion the low- and high-spin states are singlet and undecaplet, respectively. Therefore, obtaining a good estimate of this energy difference is a challenge for DFT methods. Recent studies[12] on the magnetic exchange interaction in $[Fe_2OCl_6]^{2-}$ using pure density functional methods computed an exchange coupling of -244 cm^{-1} (Hamiltonian $\hat{H} = -2J\ \hat{S}_1\ \hat{S}_2$), which is much larger than the experimental -134 cm^{-1}. It is interesting to analyze how hybrid functionals behave for the present systems because previous theoretical studies[13] for singlet/triplet energy differences have shown that the related magnetic exchange coupling is quite sensitive to the amount of exact exchange included in the functional.

We have two goals here: First to clarify whether two separated minima are present on the potential energy surface of the isolated $[Cl_3FeOFeCl_3]^{2-}$ dianion using theoretical calculations and, if not, to search for possible mechanisms that result in the anion bending. The second goal is to study the dianion's magnetic properties, taking into account the existence of two isomers or forms and combining experimental and theoretical hybrid density functional methods.

Results and Discussion

Structural Aspects

Fe−O−Fe Potential Energy Curve

Regarding the first goal given above, geometry optimizations of $[Cl_3FeOFeCl_3]^{2-}$, both for the high-spin ($S = 5$) and low-spin (broken symmetry) states, led to only one isomer as minimum on the potential energy surface: the linear one with the chlorine atoms in an alternate conformation (dihedral angles between planes Cl−Fe1−O and O−Fe2−Cl are 60°). The optimized geometrical parameters for the high- and low-spin states (Figure 2) show that Fe−O is longer in the former ground state (1.826 vs. 1.788 Å). Even though the optimizations of the low-spin state were performed using a broken symmetry (BS) approach and, e.g., not using a pure singlet wave function, the obtained values are in quite good agreement with those determined experimentally, which range from 1.752 to 1.765 Å.[3,6,7] Moreover, the computed harmonic vibrational frequencies provide an asymmetric Fe−O−Fe stretching frequency of 861 cm^{-1}, which is in very good agreement with

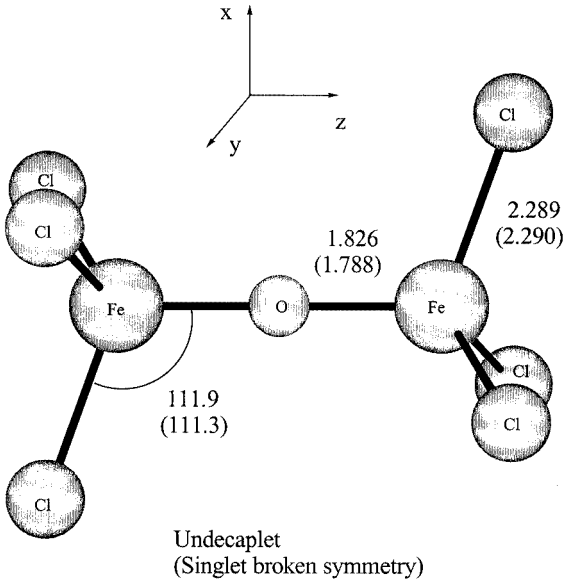

Figure 2. B3LYP-optimized geometries for the undecaplet and singlet (broken symmetry, in parentheses) ground states; distances are in Å and angles in °

that determined experimentally for several (μ-oxo)diiron complexes (850−880 cm^{-1}). In fact, intense IR absorption in this region is commonly used as a diagnostic criterion to identify monooxo-bridged Fe^{III} complexes.[3,14]

The Fe−O−Fe angular dependence has been analyzed by optimizing the geometry of the anion $[Cl_3FeOFeCl_3]^{2-}$ at different Fe−O−Fe angles (from 180.0 to 130.0°). We have considered both the in-plane (*xz*) and out-of-plane (*yz*) Fe−O−Fe bending. Figure 3 shows that for both the high- and low-spin states the energy slightly increases as the angle is reduced and that no minimum is found at about 140.0°. This behavior is similar to that found in a previous theoretical study.[10] Conversely, the energy cost for the in-plane Fe−O−Fe bending, from 180.0 to 140.0°, is < 3 kcal/mol for the singlet (BS) and < 2 kcal/mol for the undecaplet; indicating a very flat potential energy surface along this direction. The energy cost is even smaller for the out-of-plane bending. Therefore, the presence of two forms, linear and angular, in $([BzlMe_3N]^+)_2$ $[Cl_3FeOFeCl_3]^{2-}$ seems to be due not to electronic effects but probably to packing effects in the crystal.

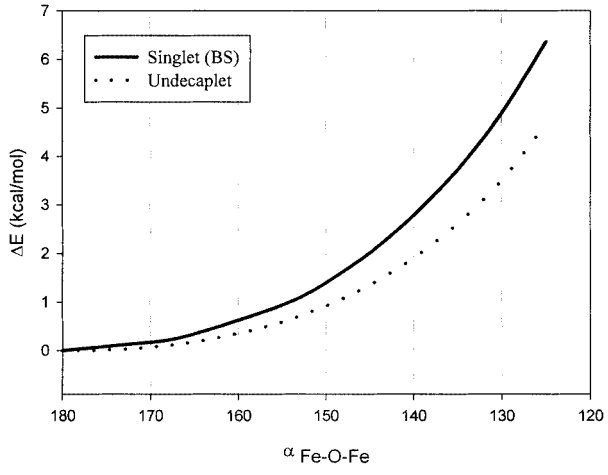

Figure 3. Relative energies of the singlet (BS) (—) and undecaplet (···) states as a function of O−Fe−O angle; in-plane bending (*xz*)

Crystal Packing Effects

The molecular structure, as well as the Mössbauer and vibrational spectroscopy results, of **2** have been reported previously.[8] However, the crystal packing effects were not analyzed. The crystal packing can be rationalized as a parallel piling of waved sheets along the unique axis *b* (Figure 4). Rows along the *a* axis can be distinguished within each sheet; they are formed of alternating cations and anions. In the five rows depicted in Figure 4 the linear anions lie in the odd ones whereas the angular ones are in the even ones. Although the neighborhood of each anion seems to be very similar, only O4 of the angular anion is involved in hydrogen bonds (numbering of ref.[8]). For symmetry reasons, this oxygen atom is bonded to two HC′3 atoms, which ride on their respective CC′ atoms. Then, while the geometry around O8 is strictly linear, for symmetry reasons, O4 has a tetrahedral bonding scheme

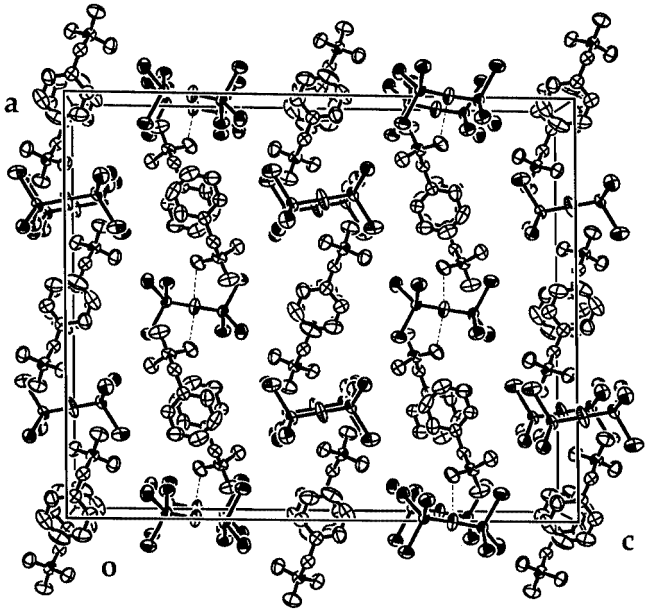

Figure 4. Perspective view of the crystal packing of **2** along the unique axis *b*

(Fe1−O4−Fe1 144.6°, HC′3···O4···HC′3 95°), with their lone pairs roughly pointing to the hydrogen atoms. These two hydrogen bonds, indicated by dashed lines in Figure 4, stabilize the angular conformation of this anion. To estimate the energy involved in this stretching process, the Espinosa model can be used.[15]

As is well known, the position of the hydrogen atoms obtained from conventional X-ray diffraction experiments are biased to their riding atom due to the polarization of the bond and the absence of core electrons in the hydrogen atoms. A correction of this effect[16] available in the PARST program[17] reduces HC′3···O4 from 2.712(6) to 2.603 Å. Introducing this value into the expression of the dissociation energy, D_e, of the Espinosa model gives 0.5 kcal/mol. As O4 is involved in two such hydrogen bonds, the energy afforded by the hydrogen bonds to distort the anion is about 1 kcal/mol, which is in close agreement with the theoretical value obtained from the potential energy curve (Figure 3), and within the range of previous estimations for CH···O hydrogen bonds.[18]

The intermolecular contacts involving the O atom in the $[Cl_3FeOFeCl_3]^{2-}$ anion were then analyzed in a set of structures[3,5−7] taken from the Cambridge Structural Database.[19] The set was formed by 17 structures selected to have no disorder and $R \leq 0.07$. In the 21 $[Fe_2OCl_6]^{2-}$ anions included in the structure set, the environment of the O atom was analyzed. The results allow the structures to be classified as three groups, showing the correlation between Fe−O−Fe angle and the presence of intermolecular interactions involving the O atom (Table 1).

Group I corresponds to anions in the bent configuration that show one or two C−H···O hydrogen bonds. Group III corresponds to linear configurations, and the intermolecular contacts, if they exist, involve pairs of short contacts related by symmetry and situated in opposite directions at

Table 1. Fe−O−Fe angle and intermolecular C···O distances in the set of 21 $[Fe_2OCl_6]^{2-}$ anions, which are classified in three groups depending on the three O-atom environments (*: corresponds to two contacts with the same C···O distance due to the crystal symmetry)

Group	Structure	Fe−O−Fe angle [°]	Shortest intermolecular C···O distances [Å]
I	DEKHUW01	148.06	3.432, 3.789
	FEDMSC01	146.54	3.547, 3.836
	SIRBAW	147.68	3.460, 3.641, 3.947
	TIQNEM	145.16	3.610, 3.653
	UBENUK	144.58	3.607
	YAFQOL01	146.42	3.430
II	COPTUW	162.14	3.683, 3.734*
	FACTEI	160.17	3.654, 3.918
	NADTAN	164.80	3.813, 3.899, 3.956
	PYDCFO	155.65	3.960
	SUJWEZ	170.23	3.987
	YAFQOL	167.87	3.566, 3.705, 3.771
III	BUTROX	180.00	3.817*
	HEBTEN	180.00	no contact
	HIRTIL	180.00	no contact
	HIRTIL	180.00	no contact
	ICAHUP	180.00	no contact
	KEBYOF	180.00	no contact
	UBENUK	180.00	no contact
	XEDHAP	180.00	3.699*
	YAFQOL01	180.00	3.977*

both sides of the anion. In group II, consisting of anions halfway between those of groups I and III, the Fe−O−Fe angles are in the range 155−170° and the intermolecular contacts are very weak or they pull the oxygen atom from different directions (Figure 5).

Thus, there is a clear dependence between intermolecular interactions and anion configuration. In group I, where the interactions are strong and cooperative, the oxygen atom is displaced from its center position and bending is produced. In group II the interactions are weak or non-cooperative, and the bending is smaller. Finally, in group III there are no interactions or they are opposed and the configuration remains linear at the potential minimum.

Magnetic Behavior

Calculation of the Magnetic Coupling Constants

The magnetic behavior of a complex can be analyzed by using the Heisenberg−Dirac−Van Vleck HDVV spin hamiltonian, where J is the magnetic coupling constant and $\hat{S}_1$ and $\hat{S}_2$ are the spin operators of the magnetically interacting centers 1 and 2 [Equation (1)].

$$\hat{H}_{HDVV} = -2J\hat{S}_1\hat{S}_2 \quad (1)$$

The magnetic coupling constant, which is positive for a ferromagnetic interaction, can be obtained from the energy differences of pure spin sates, by using ab initio configuration interaction procedures [Equation (2)].

$$E(S-1) - E(S) = 2JS \quad (2)$$

Alternatively, one can also efficiently determine magnetic coupling constants by performing unrestricted density functional calculations. However, due to the single determinant nature of the Kohn−Shan procedure, the low-spin state must be treated using the broken symmetry approach, in which the open-shell magnetic orbitals are localized in different centers, with the magnetic electrons having opposite spins. The broken symmetry approach does not lead to a pure spin state and so it is necessary to relate the energy of the broken symmetry solution to that of the pure state.[11a] For a system with two magnetic centers with spins S_1 and S_2, and considering that the overlap between magnetic orbitals is very small (weak bonding regime), J can be obtained by Equation (3).[21]

$$J = \frac{E(Broken-symmetry) - E(high-spin)}{4S_1S_2} \quad (3)$$

For the system considered here, $[Fe_2Cl_6O]^{2-}$, both Fe ions carry a local high spin of $S = 5/2$. The two centers can couple ferromagnetically to give an overall high-spin state with $S = 5$ or antiferromagnetically to provide a low-spin $S = 0$ singlet state. Whereas the high-spin state (undecaplet) can be reasonably described by a single determinant, for the low-spin state (singlet) we have used the broken symmetry approach and the magnetic coupling constant has been obtained according to Equation (4).

$$J = \frac{E(Broken-symmetry) - E(S=5)}{25} \quad (4)$$

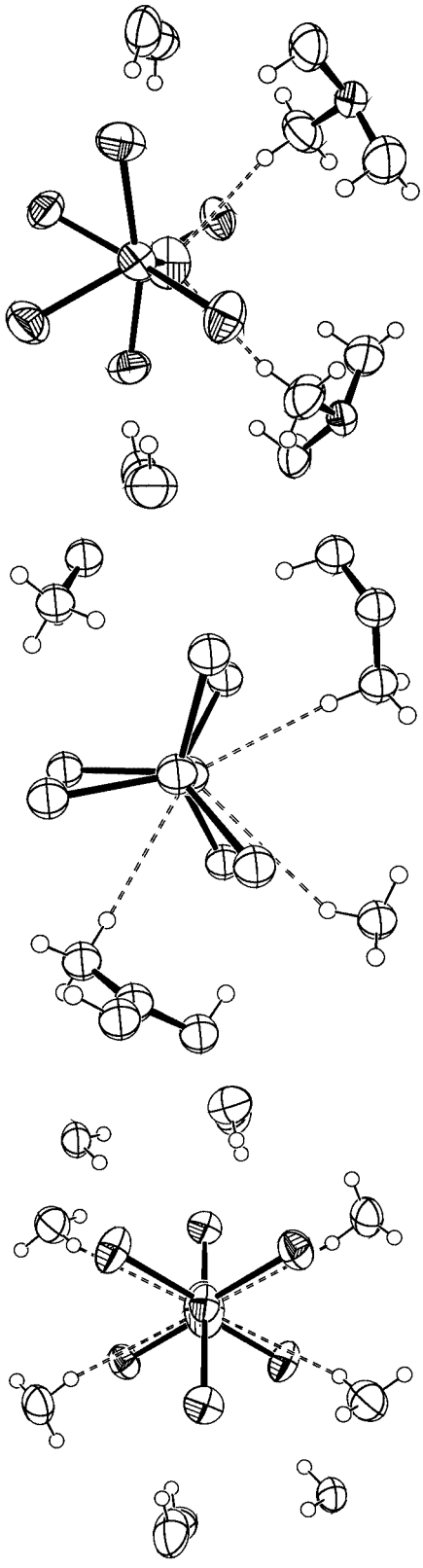

Figure 5. Perspective view of the oxygen environment of $[Cl_3FeOFeCl_3]^{2-}$ anions in a plane perpendicular to the Fe···Fe direction of representative examples of each bending-degree group: a) I, b) II and c) III; a) and c) show the two anions in **2** and b) corresponds to the NADTAN structure; diagrams generated with ORTEP-3 for Windows[20]

In addition to the B3LYP density functional approach, we have also performed calculations using the BHLYP method as previous theoretical studies have shown that the magnetic coupling constant is strongly dependent on the amount of exact exchange introduced in the functional.[13]

The magnetic coupling constants for the linear and angular forms have been computed at the experimentally determined geometry of **2**, using Equation (4). All the performed calculations indicate that antiferromagnetic exchange coupling is the most favorable interaction. Table 2 shows the computed values of J at the B3LYP and BHLYP levels for the two forms. Further enlarging the basis set in the calculation at the B3LYP level had a very small effect on the coupling constant. In contrast, the J value strongly depends on the amount of exact exchange introduced in the used functional. The value determined with the BHLYP functional, for which the amount of exact exchange is 50%, is about half of that obtained using the B3LYP functional with a ca. 20% mixture of exact exchange. Moreover, the B3LYP value is much smaller (in absolute value) than that reported recently[12] using pure density functional methods (-244 cm^{-1}). Similar behavior observed for other complexes has been attributed to the tendency of LDA and even GGA to overstabilize the antiferromagnetic coupling. This trend has been related to an overestimation of the delocalization of the spin density, which is reduced by increasing the percentage of Hartree−Fock mixture in the exchange functional.[13] Spin densities on the metal for the low-spin broken symmetry solution at the B3LYP (3.9) and BHLYP level (4.2) confirm this fact.

Table 2. Magnetic coupling constants [cm^{-1}] for the linear and angular forms at different levels of theory

Method	J_{lin}	J_{ang}
B3LYP/B1	−161	−145
B3LYP/B2	−160	−145
BHLYP/B1	−84	−73
Experimental[a]	−133	−117
	(−130)	(−119)

[a] From the magnetic susceptibility fitting by using the B3LYP/B1 (BHLYP/B1) $J_{ang} - J_{lin}$ difference.

It is also worth noting that the magnetic coupling constant of the linear form is larger than the angular one. This is not due to the different Fe−O−Fe angle, since calculations show a very small dependence of J with the Fe−O−Fe angle,[10] in agreement with experimental observations.[3] The observed difference arises from the different Fe−O distances, which are larger in the angular form due to the larger repulsive interactions between the chlorine atoms. Previous theoretical studies have shown that the absolute value of J decreases sharply as the Fe−O distance increases.[10,12]

Magnetic Measurements

The sample magnetization can be understood as a result of the magnetic coupling among the iron spins. Iron atoms

in **2** are in the ferric valence state Fe^{3+}, as confirmed by Mössbauer spectroscopy,[8] and are in a distorted tetrahedral environment. The unpaired ferric spins are coupled through the bridging oxygen atom, with the ground state corresponding to an antiferromagnetic spin interaction.

The magnetic susceptibility of powdered samples, $\chi(T)$, has been measured from 5 to 300 K by using a SQUID magnetometer (Figure 6).

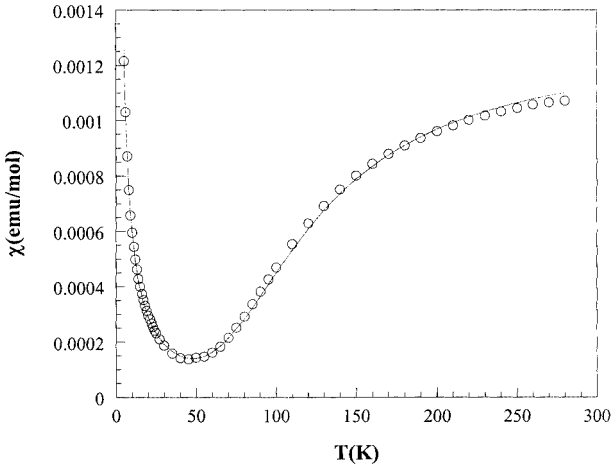

Figure 6. Magnetic susceptibility of compound **2**; the solid line corresponds to the fitting using Equation (5)

The hyperbolic tail in the low-temperature range has been attributed to paramagnetic impurities and treated as a free parameter in fitting the experimental data. After the fitting, the amount of paramagnetic impurities in the sample turns out to be only ca. 0.13 wt%.

The antiferromagnetic nature of the $[Fe_2Cl_6O]^{2-}$ anion is clearly established in the literature and is usually described by Equation (5).[22]

$$\chi_M = \frac{Ng^2\beta^2}{kT}\left[\frac{2e^{2x}+10e^{6x}+28e^{12x}+60e^{20x}+110e^{30x}}{1+3e^{2x}+5e^{6x}+7e^{12x}+9e^{20x}+11e^{30x}}\right](1-p)+p\frac{35N\beta^2}{k(T-\theta)} \quad (5)$$

In Equation (5), p represents the fraction of the paramagnetic impurity,[3] $x = J/k_BT$, J being the intensity of the magnetic coupling. The g value was fixed to 2.00 in all cases and the only fitting parameters were J, P, and θ. Because two different forms with different Fe−O−Fe bonding angles exist, namely 180 and 144.6°, it was not possible to reach an acceptable fitting of the experimental data using a single coupling constant.

The solid line in Figure 6 corresponds to the fitting of the experimental data using Equation (5), but assuming two equally weighted contributions (J_{ang} and J_{lin}) that correspond to the two different forms. As the strong correlation between the coupling constants impedes an independent determination of either of them separately, we used the computed B3LYP/B1 differences between them ($J_{ang} - J_{lin} = 16$ cm^{-1}) to obtain $J_{ang} \approx -117$ cm^{-1} and $J_{lin} \approx -133$ cm^{-1}. Even though the J values significantly depend on the density functional approach used, we expect the difference between coupling constants to be less sensitive and more accurate than the absolute values. The BHLYP values are about half of the B3LYP ones, but the $J_{ang} - J_{lin}$ differences at this level of theory (11 cm^{-1}) is only 5 cm^{-1} smaller.

By using the BHLYP computed difference as the starting point for the magnetic susceptibility fitting, the obtained coupling constants are $J_{ang} \approx -119$ cm^{-1} and $J_{lin} \approx -130$ cm^{-1} and the quality of the fitting is practically the same as that obtained with the B3LYP values. This concordance confirms the validity of the procedure used to determine the magnetic coupling constants from the fitting of the susceptibility. These values lie within the B3LYP and BHLYP values, and even the B3LYP results are in better agreement with that obtained from the fit; the BHLYP values cannot be disregarded.

These results seem to indicate that, at least for this system, a functional with an exact exchange mixing between BHLYP and B3LYP will provide results in close agreement with experiment. Unfortunately, it is not easy to know a priori how much exact exchange needs to be included in the functional to obtain an accurate answer.

Conclusion

Two different forms (bent and linear) of $[Cl_3FeOFeCl_3]^{2-}$ anions coexist in the crystal structure of $(BzlMe_3N)_2^+[Fe_2OCl_6]^{2-}$. Theoretical calculations for the low- and high-spin state of the dianion indicate that only the linear isomer is a minimum on the potential energy surface, although the energy cost for Fe−O−Fe bending is small. A detailed analysis of the crystal packing shows that the oxygen atom of the angular form is involved in two O···HC hydrogen bonds with the $BzlMe_3N$ cation. Therefore, the presence of both linear and angular forms in $([BzlMe_3N]^+)_2$ $[Fe_2OCl_6]^{2-}$ is due to crystal packing rather than electronic effects.

Moreover, analysis of those crystal structures showing bent conformations (Fe−O−Fe angle < 160°) of (μ-oxo)bis-[trichloroferrate(III)] anions shows that the bridging O atom is always involved in at least one intermolecular attractive contact. This contact, although soft, affords enough tension to bend the Fe−O−Fe angle, because the angle potential is flat, while the bulky $FeCl_3$ groups remain anchored in the crystal. The steric contribution to the Fe−O−Fe bending, related to the accommodation of the cation in the anion network holes, which is driven by attractive and repulsive contacts to chlorine atoms, must be included. The very shallow minimum of the Fe−O−Fe angle potential also explains the large vibration of oxygen atoms in the linear conformations.

The magnetic properties of $[Fe_2OCl_6]^{2-}$ have been investigated both experimentally and theoretically. The coexistence of the two forms prevented an acceptable fitting of the magnetic susceptibility when a single coupling constant was used. However, a good fit was possible by assuming two equally weighted contributions (J_{ang} and J_{lin}) that corre-

spond to the two different forms, and by considering $J_{ang} - J_{lin}$ determined by theoretical calculations. The J_{ang} and J_{lin} values were found to be −117 and −133 cm^{-1}, respectively, and are in reasonably good agreement with those obtained with the B3LYP density functional approach (−145 and −161 cm^{-1}). Considering the low computational cost of density functional methods, compared to conventional post-Hartree−Fock ones, B3LYP appears to be an efficient tool to estimate magnetic coupling constants in such systems.

Experimental Section

General: The magnetic susceptibility of the powder samples, $\chi(T)$, was measured by using a commercial SQUID magnetometer (Quantum Design MPMS-5T), over the temperature range 5−300 K, under an applied field of 5 kOe. Corrections for the diamagnetic response of the sample holder and for the diamagnetic contribution of the samples (Pascal's constants) were carried out.

Computational Details: Calculations were performed using the nonlocal hybrid three-parameter B3LYP density functional method[23] and the following basis sets. For O and Cl we used the Dunning's (9s5p)/[4s2p] and (11s7p)/[6s4p] sets,[24] respectively, supplemented with one d polarization function (ζ = 0.85 for oxygen and ζ = 0.60 for chlorine). The Fe basis set is the [8s4p3d] contraction of the (14s9p5d) primitive set of Wachters[25] supplemented with two diffuse p and one diffuse d functions,[26] the final basis sets were of the form (14s11p6d)/[8s6p4d]. This basis set is referred as Basis1 (B1). To check the effect of further enlarging the basis set, in some calculations the metal basis set was increased by adding one f polarization function,[27] i.e. based on a three-term fit to a Slater orbital of exponent 3.6, and the Cl and O atom basis sets were supplemented with one valence diffuse function. This basis set is referred as Basis2 (B2). The *J* calculations were performed using both the B3LYP and BHLYP[28] density functional methods. All calculations were performed with the Gaussian 98 package.[29]

Acknowledgments

Financial support from MEC and MCyT of Spain (Projects BQU2002-04002, PB98-0916-C02-01, PB98-0912, and MAT2000-2016) and Generalitat de Catalunya (Projects SGR2001-0181 and SGR2001-0335) is gratefully acknowledged. Professor Y. Jean (Orsay) is also acknowledged for helpful discussions.

[1] [1a] D. M. Kurtz, *Chem. Rev.* **1990**, *90*, 585−606. [1b] S. M. Gorun, S. J. Lippard, *Inorg. Chem.* **1991**, *30*, 1625−1630.
[2] R. M. Davydov, S. Ménage, M. Fontecave, A. Gräslund, A. Ehrenberg, *J. Biol. Inorg. Chem.* **1997**, *2*, 242−255.
[3] G. Haselhorst, K. Wieghardt, S. Keller, B. Schrader, *Inorg. Chem.* **1993**, *32*, 520−525 and references cited therein.
[4] D. Gatteschi, R. Sessoli, A. Cornia, *Chem. Commun.* **2000**, 725−732.
[5] M. G. B. Drew, V. McKee, S. M. Nelson, *J. Chem. Soc., Dalton Trans.* **1978**, 80−84.
[6] [6a] H. Schmidbaur, C. E. Zybill, D. Neugebauer, *Angew. Chem. Int. Ed. Engl.* **1983**, *22*, 156−157. [6b] K. Dehnicke, H. Prinz, W. Massa, J. Pebler, R. Z. Schmidt, *Anorg. Allg. Chem.* **1983**, *499*, 20−30. [6c] P. C. Healy, B. W. Skelton, A. H. White, *Aust. J. Chem.* **1983**, *36*, 2057−2064. [6d] W. M. Reiff, E. H. Witten, K. Mottle, T. F. Brennan, A. R. Garafalo, *Inorg. Chim. Acta* **1983**, *77*, L83−L88. [6e] L. Huang, F. Jiang, J. Lu, *Huaxue Tongbao* **1984**, 14; *Chem. Abstr.* **1984**, *101*, 63979a. [6f] V. I. Ponomarev, L. D. Arutyunyan, L. O. Atovmyan, *Kristallografiya* **1984**, *29*, 910−922. *Sov. Phys. Crystallog.* **1984**, *29*, 538. [6g] H. Weiss, J. Sträle, *Z. Naturforsch., Teil B* **1984**, *39*, 1453−1455. [6h] J. C. A. Boeyens, F. B. D. Khan, E. W. S. Neuse, *S. Afr. J. Chem.* **1984**, *37*, 187−192. [6i] E. W. Neuse, F. B. W. Khan, K. Berhalter, U. Thewalt, *J. Crystallogr. Spectrosc. Res.* **1986**, *16*, 483−493. [6j] P. Carty, K. C. Clare, J. R. Creighton, E. Metcalfe, E. S. Raper, H. M. Dawes, *Inorg. Chim. Acta* **1986**, *112*, 113−117. [6k] D. Petridis, A. Terzis, *Inorg. Chim. Acta* **1986**, *118*, 129−134. [6l] G. J. Bullen, B. J. Howlin, J. Silver, B. W. Fitzsimmons, I. Sayer, L. F. Larkworthy, *J. Chem. Soc., Dalton Trans.* **1986**, 1937−1940. [6m] I. Vasilevsky, R. E. Stenkamp, E. C. Lingafelter, N. J. Rose, *J. Coord. Chem.* **1988**, *19*, 171−187. [6n] S. Bernès, F. Sécheresse, Y. Jeannin, *Inorg. Chim. Acta* **1992**, *194*, 105−112.
[7] [7a] I. G. Gusakova, S. I. Pirumova, N. S. Ovanesyan, N. I. Golovina, R. F. Tofimova, G. V. Shilov, E. A. Lavrent'eva, *Zh. Obshch. Khim.* **1996**, *66*, 1436−1443. [7b] R. D. Köhn, G. Seifert, G. Kociok-Köhn, *Angew. Chem. Int. Ed. Engl.* **1997**, *35*, 2879−2881. [7c] M. James, H. Kawaguchi, K. Tatsumi, *Polyhedron* **1997**, *16*, 4279−4282. [7d] N. Kuhn, H. Kotowski, C. Maichle-Moessmer, U. Abram, *Z. Anorg. Allg. Chem.* **1998**, *624*, 1653−1656. [7e] I. Ondrejkovicová, T. Lis, J. Mrozinski, V. Vancová, M. Melník, *Polyhedron* **1998**, *17*, 3181−3192. [7f] I. G. Gusakovskaya, S. I. Pirumova, N. I. Golovina, R. F. Trofimova, G. V. Shilov, N. S. Ovanesyan, E. A. Lavrent'eva, *Russ. J. Gen. Chem.* **1999**, *69*, 175−181. [7g] B. Yan, Z.-D. Chen, S.-X. Wang, *J. Chin. Chem. Soc. (Taipei)* **2000**, *47*, 1211−1214. [7h] S. Ameerunisha, J. Schneider, T. Meyer, P. S. Zacharias, E. Bill, G. Henkel, *Chem. Commun.* **2000**, 2155−2156.
[8] E. Molins, A. Roig, C. Miravitlles, M. Moreno-Mañas, A. Vallribera, N. Gálvez, N. Serra, *Struct. Chem.* **1998**, *9*, 203−208.
[9] H. Senda, S. Kitoh, T. Suganami, K.-K. Kunimoto, *Anal. Sci.* **2000**, 1003−1004.
[10] J. R. Hart, A. K. Rappé, S. M. Gorun, T. H. Upton, *Inorg. Chem.* **1992**, *31*, 5254−5259.
[11] [11a] F. Illas, I. de P. R. Moreira, C. de Graaf, V. Barone, *J. Phys. Chem.* **1997**, *101*, 1526−1531. [11b] E. Ruiz, P. Alemany, S. Alvarez, J. Cano, *J. Am. Chem. Soc.* **1997**, *119*, 1297−1303. [11c] J. Cano, P. Alemany, S. Alvarez, M. Verdaguer, E. Ruiz, *Chem. Eur. J.* **1998**, *4*, 476−484.
[12] Z. Chen, Z. Xu, L. Zhang, F. Yan, Z. Lin, *J. Phys. Chem. A* **2001**, *105*, 9710−9716.
[13] [13a] J. Cabrero, N. Ben Amor, C. de Graaf, F. Illas, R. Caballol, *J. Phys. Chem. A* **2000**, *104*, 9983−9989. [13b] C. de Graaf, I. de P. R. Moreira, F. Illas, R. L. Martin, *Phys. Rev. B* **1999**, *60*, 3457−3464.
[14] P. Gomez-Romero, E. H. Witten, W. M. Reiff, G. B. Jameson, *Inorg. Chem.* **1990**, *29*, 5211−5217.
[15] E. Espinosa, E. Molins, C. Lecomte, *Chem. Phys. Lett.* **1998**, *285*, 170−173.
[16] G. A. Jeffrey, L. Lewis, *Carbohydr. Res.* **1978**, *60*, 179−182.
[17] [17a] M. Nardelli, *Comput. Chem.* **1983**, *7*, 95−98. [17b] M. Nardelli, *J. Appl. Crystallogr.* **1995**, *28*, 659.
[18] J. Steiner, *Angew. Chem. Int. Ed.* **2002**, *41*, 48−76.
[19] F. H. Allen, *Acta Crystallogr., Sect. B* **2002**, *58*, 380−388.
[20] L. J. Farrugia, *J. Appl. Crystallogr.* **1997**, *30*, 565.
[21] [21a] L. Noodleman, *J. Chem. Phys.* **1981**, *74*, 5737−5743. [21b] L. Noodleman, E. R. Davidson, *Chem. Phys.* **1986**, *109*, 131−143. [21c] T. Onishi, Y. Takano, Y. Kitagawa, T. Kawakami, Y. Yoshioka, K. Yamaguchi, *Polyhedron* **2001**, *20*, 1177−1184.
[22] C. J. O'Connor, *Prog. Inorg. Chem.* **1982**, *29*, 203−283.
[23] [23a] A. D. Becke, *J. Chem. Phys.* **1993**, *98*, 5648−5652. [23b] C. Lee, W. Yang, R. G. Parr, *Phys. Rev. B* **1988**, *37*, 785−789.
[24] T. H. Dunning, P. J. Hay, *Modern Theoretical Chemistry* (Ed.: H. F. Schaefer III), Plenum, New York, **1976**, vol 3, p.1.
[25] A. J. H. Wachters, *J. Chem. Phys.* **1970**, *52*, 1033−1036.

[26] P. J. Hay, *J. Chem. Phys.* **1977**, *66*, 4377−4384.
[27] C. W. Jr. Bauschlicher, S. R. Langhoff, H. Partridge, L. A. Barnes, *J. Chem. Phys.* **1989**, *91*, 2399−2411.
[28] A. D. Becke, *J. Chem. Phys.* **1993**, *98*, 1372−1377.
[29] M. J. Frisch, G. W. Trucks, H. B. Schlegel, G. E. Scuseria, M. A. Robb, J. R. Cheeseman, V. G. Zakrzewski, J. A. Montgomery, Jr., R. E. Stratmann, J. C. Burant, S. Dapprich, J. M. Millam, A. D. Daniels, K. N. Kudin, M. C. Strain, O. Farkas, J. Tomasi, V. Barone, M. Cossi, R. Cammi, B. Mennucci, C. Pomelli, C. Adamo, S. Clifford, J. Ochterski, G. A. Petersson, P. Y. Ayala, Q. Cui, K. Morokuma, D. K. Malick, A. D. Rabuck, K. Raghavachari, J. B. Foresman, J. J. V. Cioslowski, A. G. Ortiz, B. B. Baboul, G. Stefanov, A. Liu, Liashenko, P. Piskorz, I. Komaromi, R. Gomperts, R. L. Martin, D. J. Fox, T. Keith, M. A. Al-Laham, C. Y. Peng, A. Nanayakkara, C. Gonzalez, M. Challacombe, P. M. W. Gill, B. Johnson, W. Chen, M. W. Wong, J. L. Andres, C. Gonzalez, M. Head-Gordon, E. S. Replogle, J. A. Pople, *Gaussian 98, Revision A.7*, Gaussian, Inc., Pittsburgh PA, **1998**.

Received June 3, 2003
Early View Article
Published Online October 2, 2003

